

1 **Air-sea gas transfer in a shallow, flowing and coastal environment**  
2 **estimated by dissolved inorganic carbon and dissolved oxygen analyses**

3  
4 Osamu ABE<sup>1,\*</sup>, Atsushi WATANABE<sup>2</sup>, VVSS SARMA<sup>3</sup>, Yohei MATSUI<sup>4</sup>,  
5 Hiroya YAMANO<sup>5</sup>, Naohiro YOSHIDA<sup>6</sup>, AND Toshiro SAINO<sup>7,8</sup>

6 <sup>1</sup> Graduate School of Environmental Studies, Nagoya University, 464-8601 Nagoya, Japan

7 <sup>2</sup> Graduate School of Information Science and Engineering, Tokyo Institute of Technology, 152-8552  
8 Tokyo, Japan

9 <sup>3</sup> National Institute of Oceanography, 176 Lawsons Bay Colony, Visakhapatnam-17, India

10 <sup>4</sup> School of Earth Science, Ohio State University, Columbus, OH43210, USA

11 <sup>5</sup> National Institute of Environmental Studies, 305-8506 Tsukuba, Japan

12 <sup>6</sup> Interdisciplinary Graduate School of Science and Engineering, Tokyo Institute of Technology, 226-8502  
13 Yokohama, Japan

14 <sup>7</sup> Institute of Observational Research for Global Change, Japan Agency for Marine-Earth Science and  
15 Technology, 237-0061, Yokosuka, Japan

16 <sup>8</sup> Japan Science and Technology Agency, 332-0012, Kawaguchi, Japan

17

18 **Corresponding author**

19 Osamu ABE

20 Email: osamu.abe@nagoya-u.jp

21 Tel. +81-52-789-3470

22 Fax. +81-52-789-3436

23

1 **ABSTRACT**

2 We estimated gas exchange rates in Kabira Reef at Ishigaki Island, southwest  
3 Japan, using mass balance calculation with dual “biological” tracers; dissolved  
4 inorganic carbon (DIC) and dissolved oxygen (DO). With the results during nighttime,  
5 we could obtain reasonable gas transfer velocity  $k_w$  values, all of which exceeded those  
6 obtained in wind-dominant studies. The difference is likely due to the contribution of  
7 turbulence generated by the interaction of the current and bottom topography. The  
8 obtained  $k_w$  during high tides is consistent with that by Raymond and Cole (2001),  
9 whereas  $k_w$  during low tides shows higher, which seems to be caused by enhanced  
10 friction with the bottom of the reef or bubble-induced gas transfer by wave breaking at  
11 the reef crest.

12 *Keywords. Coral reef; gas transfer velocity; dissolved inorganic carbon; dissolved*  
13 *oxygen*

14  
15 **Introduction**

16 The primary controls on the air-water transfer of oxygen or other low-solubility  
17 gases in coastal waters are the current, bottom topography and wind stress. Wind stress  
18 dominates turbulence in the surface aqueous boundary layer of all systems with depths  
19 greater than 10 m or wind speeds greater than  $8 \text{ m s}^{-1}$  (Raymond and Cole 2001).  
20 Considerable efforts have gone into determining empirical relationships (Liss and  
21 Merlivat 1986; Wanninkhof 1992; Wanninkhof and McGillis 1999; Nightingale et al.  
22 2000). On the other hand in shallower, flowing circumstances, even surface turbulence  
23 can be dominated by the interaction of the current with bottom topography, and both  
24 observational and experimental data are comparatively limited (Upstill-Goddard 2006).

1 Physical controls on gas transfer in shallow, flowing coral reef platforms fall  
2 somewhere between these two extremes, and both wind and hydrologically induced  
3 turbulence can be important, depending in part on the depth and width of the system and  
4 in part on the velocity of tidal or river flows (Marino and Howarth 1993).

5 Several methods are used to determine air-water gas transfer velocity in natural  
6 water systems. Purposeful gas tracer techniques (e.g., SF<sub>6</sub>), which provide the least  
7 equivocal answer, are the most promising for natural water studies. Clark et al. (1994)  
8 applied this method (SF<sub>6</sub> and <sup>3</sup>He) to unidirectional water flow system like the Hudson  
9 River. This approach was rarely used to more complex flow systems like estuaries, coral  
10 reefs. Many experiments to determine gas exchange rates in coastal environments have  
11 been conducted using the “helmet” method (Clark et al. 1994), in which the gas  
12 exchange rate is calculated from the rate of gas accumulation into an inverted dome  
13 floating on the water surface. The major problem is the degree to which the floating  
14 dome disturbs the surface turbulence regime; the physical driving force behind the gas  
15 exchange is unknown. Laboratory experiments have found little agreement between gas  
16 exchange rates determined by the helmet method and other approaches (Clark et al.  
17 1994). Recently, Tokoro et al. (2007, 2008) examined and evaluated this method by  
18 comparing the energy dissipation rates measured inside and outside the floating  
19 chamber and confirmed that there was no significant disturbance to the surface  
20 turbulence regime. Aqueous turbulence analysis (micrometeorological technique) is also  
21 being common method to determine gas transfer velocity in the coastal waters. Zappa et  
22 al. (2003, 2007) combined various techniques to measure surface turbulence (surface  
23 renewal rates, turbulent scales, and energy dissipation rates).

24

1           Mass balance calculation is an alternative method (e.g. Marino and Howarth  
2 1993; Cai et al. 1999), however, the magnitude and variability of the sources and sinks  
3 of the dissolved gas must be well known (Marino and Howarth 1993; Raymond and  
4 Cole 2001).

5           In this study, we estimated gas transfer velocities in the shallow, flowing and  
6 coastal environment of a coral reef platform using mass balance calculation with dual  
7 “biological” tracers; dissolved inorganic carbon (DIC) and dissolved oxygen (DO). Few  
8 studies have used these tracers to determine gas transfer velocity; however, recent  
9 progress in analytical methods measuring DIC and the relative simplicity of our field  
10 situation made their use practicable.

11           Because of their high metabolic activities, coral reefs generally have wide diel  
12 variations in DIC and DO. With regard to CO<sub>2</sub>, metabolic fluxes (photosynthesis or  
13 respiration) significantly dominate over gas exchange flux (e.g. Frankignoulle et al.  
14 1996). Thus, we postulated that the diel variation of DIC is determined solely by  
15 metabolic activity in a limited water residence time. On the other hand, DO gas  
16 exchange flux is usually comparable to that of metabolic fluxes. Based on the differing  
17 characteristics of these gases in coral reefs, we define DIC as a “biologically reactive  
18 but physically conservative” tracer and DO as a tracer “both biologically and physically  
19 reactive.” Thus, the gas transfer velocity of O<sub>2</sub> can be calculated by eliminating the  
20 estimated metabolic contribution of DIC variations.

21           Several investigations were conducted to measure DO and DIC simultaneously,  
22 mainly for open ocean environments. In the open ocean settings, DIC does not act as  
23 physically conservative tracer due to the relatively low metabolic rates. Moreover, the  
24 difference of inventory between DO and DIC in the mixed layer yields the difference of

1 equilibration time with respect to gas exchange (e.g., Nakayama et al. 2000; McNeil et  
2 al. 2006). Recently, Körtzinger et al. (2008) demonstrated long-term (1-year)  
3 observational results for DO and pCO<sub>2</sub> at the central Labrador Sea and obtained a  
4 consistent gas transfer velocity with previous studies (Wanninkhof 1992; Wanninkhof  
5 and McGillis 1999) at wind speed more than 10 m s<sup>-1</sup>, with selected observation period.

6           A mass balance calculation with biological tracers includes several  
7 uncertainties. First, the coral reef ecosystem is generally dominated by calcifying  
8 organisms as corals and calcifying algae. Although calcification decreases DIC, DO  
9 does not change. Therefore, calcification rates must be determined. They can be  
10 calculated by temporal or spatial changes of seawater total alkalinity (TA). Second, the  
11 ratios of DO change to DIC change during photosynthesis and organic matter  
12 decomposition/respiration must be defined by a photosynthetic quotient (PQ) and  
13 respiratory quotient (RQ), respectively. Third, the sites of metabolism that play roles in  
14 the tracer sources must be determined. Finally, if water advection and mixing processes  
15 are complicated, the determination of water fluxes is very difficult.

16           Kabira Reef at Ishigaki Island, southwest Japan, is an ideal location to  
17 minimize these uncertainties. The current analysis of Yamano et al. (1998) showed that  
18 the circulation pattern under calm or northern wind conditions is characterized simply  
19 by an inflow of offshore waters into the moat over the reef crest and an outflow through  
20 a prominent channel. Because most organisms are concentrated around the reef crest,  
21 the metabolism site can be easily described.

22

## 23 **MATERIALS AND METHODS**

### 24 *Study site*

1 Kabira Reef is a well-developed fringing reef located on the north coast of  
2 western Ishigaki Island, southwest Japan (Figs. 1, 2). Ishigaki Island is situated in a  
3 monsoon area, where the dominant wind direction is from the south in summer and  
4 north in winter. Yamano et al. (1998) concluded that wind direction markedly  
5 influences the seasonal patterns of water circulation at Kabira Reef. Under calm or  
6 northern wind conditions, the circulation pattern is characterized by an inflow of  
7 offshore waters into the moat over the reef crest and an outflow through a prominent  
8 channel, whereas southern wind conditions this pattern is weakened or disturbed  
9 (Yamano et al., 1998). Thus, during northern to northeastern winds, metabolic activities  
10 with respect to primary production can be observed over the entire reef, if waters from  
11 offshore and the channel are taken as the initial and final values, respectively. Figure 2  
12 shows that the trajectories of input water to Kabira Reef during the observation periods  
13 clearly reproduce the flow pattern described above.

#### 14 ***Research methods***

15 Observations were conducted on 7-8 March 2003. To calculate water  
16 mass balance, electromagnetic current meters (ACM-8M, 16M, Alec Electronics) were  
17 situated at three points and set to measure every 5 minutes (Fig. 2). The sensor-heads  
18 were set 50 cm above the bottom. At the point M800 (24°28'22.8"N, 124°8'42.5"E),  
19 the volume transport of water entering from offshore was measured; that of water  
20 exiting through the channel was measured at the point E350 (24°27'56.5"N,  
21 124°8'47.4"E). The other current meter, at the point W400 (24°28'26.9"N,  
22 124°8'17.0"E), was situated to confirm whether there was additional flow from or to  
23 northwest (parallel to the shoreline) or not. As a result, we did not observe significant  
24 NW-SE component of water flow at the W400, then current data at this site was not

1 used afterward. We also conducted drifting buoy experiments that were described by  
2 Miyajima et al. (2007) in order to determine the length of water path and its residence  
3 time in the reef. A small drogue made of a floating buoy and an underwater cross-shape  
4 plate was released near the point M800, and it was followed by the boat to determine its  
5 position using GPS. Nine experiments were conducted randomly during the observation  
6 period. Tracks of the drifting buoy were plotted in Fig. 2. Oceanographic and  
7 meteorological parameters were observed at E350. Water temperature, salinity, tidal  
8 level, and dissolved oxygen were monitored every 5 minutes by DO-CTD sensor  
9 (Hydrolab DATASONDE 4a). Salinities were calibrated by Portasal<sup>TM</sup> salinometer  
10 (Guildline Instruments) with IAPSO seawater standards and bottled seawater samples  
11 that were collected irregularly. The O<sub>2</sub> probe with membrane electrode was calibrated  
12 prior to deployment using oxygen-free (0 % in saturation) and oxygen-saturated (100 %  
13 in saturation) solutions. These solutions were measured independently by conventional  
14 Winkler titration. Sensor drift was also corrected every day by measuring saturated  
15 solution. Seawater samples for DIC and TA analysis were collected every 2-hour until  
16 0800 March 7 and 1-hour afterward in 500-ml glass bottles (DURAN®) from surface  
17 water at E350 and then poisoned using HgCl<sub>2</sub> solution. Samples from offshore were  
18 taken once a day with a same manner. DIC and TA were determined by continuous-  
19 flow through a DIC and TA analyzer developed by University of Tokyo, Japan Science  
20 and Technology Agency, and Kimoto Electronics (Kimoto et al. 2001; Watanabe et al.  
21 2004; Watanabe 2004). For DIC, the sample water was acidified with phosphoric acid,  
22 and the extracted CO<sub>2</sub> was measured using a non-dispersive infrared gas analyzer (LI-  
23 6252, LICOR). For TA, the sample water and a specific proportionate HCl solution  
24 were mixed, and the pH difference between the initial and acidified water was measured

1 using a combined glass electrode. The precisions of the water temperature, salinity, DO,  
 2 DIC and TA were 0.1 °C, 0.05 psu, 1.5, 2 and 1.5  $\mu\text{mol kg}^{-1}$ , respectively (1 S.D.). The  
 3 accuracies of the DO, DIC and TA were 3, 3 and 4  $\mu\text{mol kg}^{-1}$ , respectively. Those of the  
 4 water temperature and salinity were not evaluated in this study.

5 DIC and TA were normalized to the salinity of 35 conventionally like,

$$7 \quad \text{NDIC} = \text{DIC}^{0.35/S} \quad (\text{eq.1})$$

8  
 9 where TA is treated similarly as NTA.

10 Wind, air temperature, solar radiation, humidity, and air pressure were monitored every 5  
 11 minutes by an Aanderaa® weather station situated at E350 with the height of 5 m above  
 12 mean sea level. Horizontal wind speeds were converted to those at 10 m height by  
 13 following equations (Brutsaert, 1982).

$$15 \quad U_{10}(\text{ms}^{-1}) = \frac{u_*}{k} \ln \frac{z}{z_0}, \quad u_* = C_{d0.5} u_{\text{obs}} \quad (\text{eq.2})$$

16  
 17 where  $U_{10}$ ,  $u_*$ ,  $k$ ,  $z_0$ ,  $C_d$  and  $u_{\text{obs}}$  represent wind speed at 10 m height, friction velocity,  
 18 von Karman constant (0.4), roughness at water surface, drag coefficient and observed  
 19 wind speed at 5 m height ( $\text{ms}^{-1}$ ), respectively. Surface roughness was calculated as  $z_0 =$   
 20  $1.65 \times 10^{-4} u_{*1.4}$ , and drag coefficient of  $1.15 \times 10^{-3}$  was applied according to the study by  
 21 Emmanuel (1975).

22



## 1 **OBSERVATIONAL RESULTS**

2           Figure 3 shows a time series of meteorological and oceanographic observations  
3 at Kabira Reef on 7-8 March 2003. The average wind speed (Fig. 3a) was  $8 \text{ m s}^{-1}$  at 5 m  
4 above sea level with the dominant direction N to NNE, and the wind-driven surface  
5 flow from offshore was assumed to be constantly northern. From 1100 to 1400 on 6  
6 March, 20 mm rainfall resulted in relatively low salinity at the beginning of the  
7 observation period (Fig. 3b), after which salinity gradually increased. Salinity was  
8 almost constant throughout the observation period with tiny diel variation associated  
9 with tidal changes. Offshore salinities were constant at 34.97. The average tidal  
10 difference of 1.2 m corresponded to the middle tide toward neap (Fig. 3c). The average  
11 current direction at M800 (reef crest) was almost the same as the N to NE wind  
12 direction (Fig. 3d) and offshore water inflow over the reef crest was almost parallel to  
13 the wind direction. The direction of water exiting via the southeast channel was nearly  
14 perpendicular to the channel, and was constant throughout the observation period (Fig.  
15 3e). Dissolved oxygen was almost less than saturation during the observation period,  
16 except on 8 March (Fig. 3f), when the daytime concentration exceeded saturation level  
17 due to the increase of net productivity associated with solar radiation. DIC and DO  
18 variations were nearly symmetrical (Fig. 3g). TA was low during the daytime and close  
19 to offshore values at night (Fig. 3h). Offshore DO, NDIC and NTA were almost  
20 constant through the observation period, namely  $198, 2019$  and  $2334 \mu\text{mol kg}^{-1}$  for 0900  
21 March 7 and  $204, 2019$  and  $2339 \mu\text{mol kg}^{-1}$  for 0840 March 8, respectively. Additional  
22 offshore samples were taken for DIC and TA at 1830 March 6, and there was no  
23 significant difference from other two results as  $2017$  and  $2335 \mu\text{mol kg}^{-1}$  for NDIC and  
24 NTA, respectively.

1

2 **ESTIMATION OF GAS TRANSFER VELOCITY  $k_w$  DERIVED**  
3 **FROM DO-DIC ANALYSES**

4 Determining gas transfer velocity was a two-step process involving the  
5 calculation of 1) the residence time of reef water and 2) the metabolic rates (production  
6 and respiration rates) of reef organisms.

7

8 *Calculation of the residence time of reef water*

9 The residence time of reef water was calculated as a long section of the water  
10 path divided by the line flux of the water:

11

12  $T = (L \times D_{avg}) / (S_i \times D) \times f$  (eq.3)

13

14 where  $L$ ,  $D_{avg}$ ,  $S_i$ , and  $D$  represent the length of the path from the reef edge to the  
15 channel, spatial average water depth along the pass, current speed, and water depth at  
16 the reef edge, respectively. The  $L$  value of 1100 m was based on water trajectory results  
17 obtained from buoy experiments.  $D_{avg}$  was estimated from trajectories and topographic  
18 sections of Kabira Reef.  $S_i$  and  $D$  were derived from observed values at E350. The term  
19  $f$  is a correction factor that represents the ratio of mean water flux at the reef exit to the  
20 water flux observed at E350. This factor was determined by comparison with the actual  
21 residence time observed in the drifting buoy experiments. Figure 4 indicates both the  
22 observed and estimated residence times, indicated by the filled diamonds and solid line,  
23 respectively. Based on the three observations, we determined an  $f$  value of 0.7, which  
24 implies that the water flux at E350 was 1.4 times greater than average. This factor

1 appears to be constant throughout the observation period. The calculated residence time  
2 was 1.1 h on average, with the maximum observed at 0200 (1.5 h) and the minimum  
3 observed at 1000 (0.8 h). The relative error of  $\pm 5.8\%$  was obtained based on the  
4 precisions for depth and current measurements provided by the manufacturer. Residence  
5 time tended to be less during flood tides than at ebb tides. In a single tidal cycle,  
6 relatively higher values were observed 2 hours before and after the ebb tide.

7

### 8 *Calculation of the metabolic rates*

9           Metabolic rates (net community production; NCP) for the reef community were  
10 calculated from changes in TA and DIC between offshore and E350 (eq.4). By  
11 definition, calcification decreases TA as 2 moles per mol of  $\text{CaCO}_3$  formation, so that  
12 half of the TA changes correspond to the calcification rate for the entire reef.

13

$$14 \text{ NCP (mmol m}^{-2} \text{ h}^{-1}) = [(\text{DIC}_{\text{final}} - \text{DIC}_{\text{initial}}) - (\text{TA}_{\text{final}} - \text{TA}_{\text{initial}})/2] \times D_{\text{avg}} / T$$

15 (eq.4)

16 where  $\text{DIC}_{\text{final}}$  and  $\text{TA}_{\text{final}}$  represent the observed NDIC and NTA at E350, respectively,  
17 and  $\text{DIC}_{\text{initial}}$  and  $\text{TA}_{\text{initial}}$  represent offshore NDIC and NTA, respectively, using the  
18 average values of the two offshore seawater samplings (Fig. 3g and h). This calculation  
19 was same as that indicated by Gattuso et al. (1996), except for influence of  $\text{CO}_2$  gas  
20 exchange on metabolic rates (see discussion in detail). Daytime production on 8 March  
21 was higher than that on 7 March due to higher irradiance. Nighttime respiration differed  
22 slightly between 7 and 8 March, but was essentially constant each night. The metabolic  
23 rates we obtained agree well those obtained by Kayanne et al. (2005) in the same season  
24 at Shiraho Reef on the east coast, based on fixed-point observations during slack-water

1 periods.

2           The O<sub>2</sub> transfer flux between the atmosphere and reef water was determined  
3 using the calculated water residence time, metabolic rates and temporal DO  
4 concentration observed at E350. To convert carbon production or respiration to those of  
5 O<sub>2</sub>, we used metabolic quotients, such as the photosynthetic quotient (PQ) or respiratory  
6 quotient (RQ). Gattuso et al. (1999) obtained a uniform PQ of 1.1, based on two  
7 different reef observations, and concluded that this value agreed with previous  
8 investigations at other sites. Strickland and Parsons (1978) proposed a RQ value of 1.0  
9 for normal marine populations exposed to moderate light intensities. Several studies that  
10 estimated coral reef ecosystem RQs (Kinsey 1978; Barnes and Devereux 1984) did not  
11 find RQ to differ significantly from unity. Consequently, we used PQ (NCP > 0) and  
12 RQ (NCP < 0) values of 1.1 and 1.0, respectively. Anoxic decomposition of organic  
13 materials such as sulfate reduction, which influences not on DO but on DIC and TA  
14 alone, can be neglected. Since bottom sediments of the reef are composed mostly of  
15 coarse bioclastic sands or rubbles (fragments of coral skeletons and foraminiferal tests;  
16 Yamano et al. 2000), sedimentary environment can be regarded as oxic.

17           Finally, O<sub>2</sub> transfer flux was calculated as follows:

18

$$19 \quad G \text{ (mmol/m}^2\text{/h)} = (\text{DO}_{\text{final}} - \text{DO}_{\text{initial}}) \times D_{\text{avg}} / T - M_{\text{O}_2} \quad (\text{eq.5})$$

20

21 where M<sub>O<sub>2</sub></sub> is 1.1NCP (NCP>0) and 1.0NCP (NCP<0), respectively. We converted the  
22 obtained gas exchange flux G to gas transfer velocity k<sub>w,O<sub>2</sub></sub>, using the saturation degree  
23 of O<sub>2</sub>.

24

1  $k_{w,O_2} = G / (DO_{avg} - DO_{sat})$  (eq.6)

2

3 The  $DO_{avg}$  was determined by the average of  $DO_{initial}$  and  $DO_{final}$ , as defined in eq. (5).

4 For comparison with previous studies,  $k_{w,O_2}$  was normalized to Schmidt number of 600.

5

6  $k_{w,600} = k_{w,O_2}(600/Sc_{O_2})^{-0.5}$  (eq.7)

7  $Sc_{O_2} = 1953.4 - 128t + 3.9918t^2 - 0.050091t^3$  (eq.8)

8

9 where t represents water temperature in deg. C. Schmidt number of  $O_2$  was determined  
10 using a polynomial fitting equation by Wanninkhof (1992).

11 Total errors for estimating NCP and  $k_w$  were evaluated by summing up of  
12 relative errors for each component, then obtained as 6.5 % and 9.3 % for NCP and  $k_w$  in  
13 1 S. D., respectively.

14

## 15 **DISCUSSION**

16 Table 1 lists the estimated  $k_w$  values derived from the combined DO-DIC  
17 analysis. In general,  $k_w$  should have positive values; however, we found negative values  
18 in daytime, caused by the prescribed PQ value. Obtaining positive values for all periods  
19 required a PQ value of 0.5. If this is the case, however, several  $k_w$  values of the order of  
20 hundreds  $cm\ h^{-1}$  will be found in daytime on 8 March, which are unrealistic numbers.  
21 Several studies have found  $PQ < 1$  (Pokorny et al. 1989; Johnson et al. 1981; Pichon  
22 1985). Moreover, Burris (1981) showed a wide PQ range from 0.1 to 1.0 at oxygen  
23 concentrations greater than saturation. Our results may support this and suggest that a

1 constant PQ value is inapplicable. On the other hand, nighttime  $k_w$  values were  
2 relatively stable, implying that a constant RQ value can be applied. Consequently, the  
3 following discussion of gas transfer velocity is based on the nighttime  $k_w$  values  
4 obtained on 7 and 8 March.

5 Consistent gas transfer velocities obtained for nights of 7 and 8 March were  
6  $49 \pm 15$  and  $49 \pm 14$   $\text{cm h}^{-1}$ , respectively. The average horizontal wind speeds were 8.9 on  
7 7 March and  $8.7 \text{ m s}^{-1}$  on 8 March. All of the results exceeded the estimated wind-  
8 driven transfer velocity by four conventional algorithms (Fig. 5), clearly demonstrating  
9 the occurrence of surface turbulence created by the friction of water passing over the  
10 bottom of the reef. We divided the results into periods of higher and lower tidal levels,  
11 based on the average water depth of the trajectory (1.26 m). Except for an outlying  
12 result at 0000 7 March (upper-left in Fig. 5), the average values for high and low tides  
13 were  $43 \pm 8$  and  $52 \pm 15$   $\text{cm h}^{-1}$ , respectively. The lower water depth tended to result in  
14 greater gas transfer, although the average horizontal wind speed was slightly lower  
15 during the period ( $8.7$  at low tide and  $9.0 \text{ m s}^{-1}$  at high tide; Fig. 5).

16 As seen in Figure 5, the average value during high tides (filled square) falls on  
17 the regression curve compiled for “non-dome” studies at rivers and estuaries by  
18 Raymond and Cole (2001). However, their calculation was based on nine observations  
19 at wind speeds  $< 7 \text{ m s}^{-1}$ , whereas all of our observed wind speeds were  $> 7 \text{ m s}^{-1}$ . Thus,  
20 the curve in Fig. 5 is extrapolated but is consistent with observed results.

21 Higher values during the low tides are still unidentified, however, following  
22 two reasons seems to be possible. First, turbulence caused by bottom friction was  
23 enhanced during low tides. The solid curve in Fig. 5 was obtained without observations  
24 those had water depth less than 1 m (Raymond and Cole, 2001). In that case, the

1 turbulence created by bottom friction seems to be enhanced. Tokoro et al. (2007; 2008)  
2 also showed higher values from Fukido Reef, northern part of Ishigaki Island. They  
3 obtained significant difference of  $k_w$  between the reef and adjacent river mouth and  
4 concluded that it was caused by the difference of the bottom roughness. Second, the  
5 bubble formation due to wave breaking at the reef crest seems to be also possible. The  
6 average of significant wave height during observation periods is 0.6 m, meanwhile the  
7 average of water depth at M800 (point at the reef crest) is 0.80 m. Thus, wave breaking  
8 and associated bubble-induced gas transfer should occur during low tides. Further  
9 investigation is required to clarify the difference of  $k_w$  between high and low tides.

10 Finally, contribution of  $\text{CO}_2$  gas exchange to the DIC concentration was  
11 evaluated. At first, fugacity of  $\text{CO}_2$  ( $f\text{CO}_2$ ) in seawater was calculated by the program  
12 for  $\text{CO}_2$  system calculation (Lewis and Wallace 1998) using DIC and TA data.  
13 Dissociation constants of carbonic acid were derived from the study by Roy et al.  
14 (1993). Calculated  $f\text{CO}_2$  variation was shown in Fig. 3i, and one can see the variation  
15 was almost parallel to that of NDIC (Fig. 3g) due to the relative constancy of NTA to  
16 NDIC. It could be also seen that offshore  $f\text{CO}_2$  was almost constant through the  
17 observation period, as 367 and 371  $\mu\text{atm}$  for March 7 and 8, respectively. Most of reef  
18 water  $f\text{CO}_2$  were above the offshore value except for the daytime of March 8, however  
19 seems to be mostly below the atmospheric  $\text{PCO}_2$  value of 381  $\mu\text{atm}$ , which was monthly  
20 average observed at Yonaguni Island 100 km off the Ishigaki Island (Japan  
21 Meteorological Agency). Then  $\text{CO}_2$  flux over the entire reef was estimated with the  
22 average  $k_{w,600}$  value of 49  $\text{cm h}^{-1}$ , atmospheric  $\text{PCO}_2$  of 381  $\mu\text{atm}$  and the solubility  
23 provide by Weiss (1974). As shown in Fig. 5b (open diamonds), the entire reef system  
24 played a role of absorbing atmospheric  $\text{CO}_2$  during the observation period, however the

1 magnitude of the gas exchange flux was almost 100 times lower than metabolic rates  
2 (NCP). If this CO<sub>2</sub> flux was incorporated into the equation 2, final values of  $k_w$  would  
3 increase 0.2 in average, which was within total error of  $k_w$  estimation.

4

## 5 **CONCLUSIONS**

6 We demonstrated gas transfer velocity in a shallow, flowing coral reef  
7 environment, using mass balance calculations with two biological tracers. Using  
8 nighttime observations, we obtained reasonable gas transfer velocity  $k_w$  values, all of  
9 which exceeded those obtained in wind-dominant studies. The difference is likely due to  
10 the contribution of turbulence generated by the interaction of the current and bottom  
11 topography.

12 The obtained  $k_w$  during high tides is consistent with that by Raymond and Cole  
13 (2001), whereas  $k_w$  during low tides shows higher, which seems to be caused by  
14 enhanced friction with the bottom of the reef or bubble-induced gas transfer by wave  
15 breaking at the reef crest.

16

## 17 **ACKNOWLEDGMENTS**

18 We thank Mr. Makoto Sasaki for all his efforts of supporting in field survey.  
19 Thanks are also extended to Tatsuki Tokoro for providing  $k_w$  data. We appreciate  
20 Alberto V. Borges, an associate editor, and four anonymous reviewers for valuable and  
21 constructive comments on the manuscript. This study was supported by the Asahi  
22 Breweries Foundation (H14) and partly supported by the SORST and CREST projects  
23 (JST).



1

2 **REFERENCES**

3 Barnes, D. J. AND M. J. Devereux 1984. Productivity and calcification on a coral reef:

4 A survey using pH and oxygen electrode techniques. *Journal of Experimental*  
5 *Marine Biology and Ecology* 79: 2130-231.

6 Brutsaert, W. 1982. Evaporation into the atmosphere, Dordrecht/Boston/Lancaster. D.

7 Reidel Publishing Company, pp. 299.

8 Burris J. E. 1981. Effects of oxygen and inorganic carbon concentration on the

9 photosynthetic quotients of marine algae. *Marine Biology* 65: 215-219.

10 Cai, W. -J., L. R. Pomeroy, M. A. Moran, AND Y. Wang 1999. Oxygen and carbon

11 dioxide mass balance for the estuarine-intertidal marsh complex of five rivers in

12 the southeastern U.S. *Limnology and Oceanography* 44: 639-649.

13 Clark, J. F., R. Wanninkhof, P. Schlosser, AND H. J. Simpson 1994. Gas exchange

14 rates in the tidal Hudson river using a dual tracer technique. *Tellus* 46B: 274-285.

15 Emmanuel, C. B. 1975. Drag and bulk aerodynamic coefficients over shallow water.

16 *Boundary-Layer Meteorology* 8: 465-474.

17 Frankignoulle, M., J. P. Gattuso, R. Biondo, I. Bourge, G. Copin-Montégut, AND M.

18 Pichon 1996. Carbon fluxes in coral reefs. II. Eulerian study of inorganic carbon

19 dynamics and measurement of air-sea CO<sub>2</sub> exchanges. *Marine Ecology Progress*

20 *Series* 145: 123-132.

21 Gattuso, J. -P., M. Pichon, B. Delesalle, C. Canon, AND M. Frankignoulle 1996.

22 Carbon fluxes in coral reefs. I. Lagrangian measurement of community

23 metabolism and resulting air-sea CO<sub>2</sub> disequilibrium. *Marine Ecology Progress*

24 *Series* 145: 198-121.

- 1 Gattuso, J. -P., M. Frankignoulle, AND S. V. Smith 1999. Measurement of community  
2 metabolism and significance in the coral reef CO<sub>2</sub> source-sink debate.  
3 *Proceedings of the National Academy of Sciences of the United States of America*  
4 96: 13017-13022.
- 5 Johnson K. M., C. M. Burney, AND J. McN. Sieburth 1981. Enigmatic marine  
6 ecosystem metabolism measured by direct diel  $\Sigma$ CO<sub>2</sub> and O<sub>2</sub> flux in conjunction  
7 with DOC release and uptake. *Marine Biology* 65: 49-60
- 8 Kayanne, H., H. Hata, S. Kudo, H. Yamano, A. Watanabe, Y. Ikeda, K. Nozaki, K.  
9 Kato, A. Negishi, AND H. Saito 2005. Seasonal of bleaching-induced changes in  
10 coral reef metabolism and CO<sub>2</sub> flux. *Global Biogeochemical Cycles* 19: GB3015.
- 11 Kimoto, H., H. Kayanne, S. Kudo, K. Nozaki, A. Negishi, AND K. Kato 2001. A high  
12 time-resolution analyzer for total alkalinity of seawater, based on continuous  
13 potentiometric measurement. *Analytical Sciences* 17: i415- i418.
- 14 Kinsey, D. W. 1978. Productivity and calcification estimates using slack-water periods  
15 and field enclosures. In: *Coral reefs: research methods*, edited by D. R. Stoddart  
16 and R. E. Johannes, UNESCO, Paris, 439-468.
- 17 Körtzinger, A., U. Send, D. W. R. Wallace, J. Karstensen, AND M. DeGrandpre 2008.  
18 Seasonal cycle of O<sub>2</sub> and pCO<sub>2</sub> in the central Labrador Sea: Atmospheric,  
19 biological and physical implications. *Global Biogeochemical Cycles* 22: GB1014.
- 20 Lewis, E. AND D. W. R. Wallace 1998. Program Developed for CO<sub>2</sub> System  
21 Calculations. ORNL/CDIAC-105. Carbon Dioxide Information Analysis Center,  
22 Oak Ridge National Laboratory, U.S. Department of Energy, Oak Ridge,  
23 Tennessee.
- 24 Liss, P. S. AND L. Merlivat 1986. In: *The role of air-sea exchange in geochemical*

- 1           *cycling*, ed P. Buat-Ménard, 113-128. NATO ASI Series, Reidel, Utrecht.
- 2 Marino, R AND R. W. Howarth 1993. Atmospheric Oxygen Exchange in the Hudson  
3 River: Dome Measurements and Comparison With Other Natural Waters.  
4 *Estuaries*, 16: 433-445.
- 5 McNeil, C. L., B. Ward, W. R. McGillis, M. D. DeGrandpre, AND M. Marcinowski  
6 2006. Fluxes of N<sub>2</sub>, O<sub>2</sub>, and CO<sub>2</sub> in nearshore waters off Martha's Vineyard.  
7 *Continental Shelf Research* 26: 1281-1294.
- 8 Miyajima, T., Y. Tanaka, I. Koike, H. Yamano, AND H. Kayanne 2007. Evaluation of  
9 spatial correlation between nutrient exchange rates and benthic biota in a reef-flat  
10 ecosystem by GIS-assisted flow-tracking. *Journal of Oceanography* 63: 643-659.
- 11 Nakayama, N., S. Watanabe, AND S. Tsunogai 2000. Difference in O<sub>2</sub> and CO<sub>2</sub> gas  
12 transfer velocities in Funaka Bay. *Marine Chemistry* 72: 115-129.
- 13 Nightingale, P. D., G. Malin, C. S. Law, A. J. Watson, P. S. Liss, M. I. Liddicoat, J.  
14 Boutin, AND R. C. Upstill-Goddard 2000. In situ evaluation of air-sea exchange  
15 parameterizations using novel conservative and volatile tracers. *Global*  
16 *Biochemical Cycles* 14: 373-387.
- 17 Pichon, M 1985. Organic production and calcification in some coral reefs of Polynesia.  
18 *Proceedings of the fifth International Coral Reef Congress, Tahiti* 6: 173-177.
- 19 Pokorný, J., P. T. Orr, J. P. Ondok, AND P. Denny 1989. Photosynthetic quotients of  
20 some aquatic macrophyte species. *Photosynthetica* 23: 494-506.
- 21 Raymond, P. A. AND J. J. Cole 2001. Gas Exchange in Rivers and Estuaries: Choosing  
22 a Gas Transfer Velocity. *Estuaries* 24: 312-317.
- 23 Roy, R. N., L. N. Roy, K. M. Vogel, C. Porter-Moore, T. Pearson, C. E. Good, F. J.  
24 Millero, AND D. M. Campbell 1993. The dissociation constants of carbonic acid

1           in seawater at salinities 5 to 45 and temperatures 0 to 45°C. *Marine Chemistry* 44:  
2           249-267.

3   Strickland, J. D. H. AND T. R. Parsons 1972. A Practical Handbook of Seawater  
4           Analysis, 2nd edition. Ottawa. Fisheries Research Board of Canada.

5   Tokoro, T., A. Watanabe, H. Kayanne, K. Nadaoka, H. Tamura, K. Nozaki, K. Kato,  
6           AND A. Negishi 2007. Measurement o air-water CO<sub>2</sub> transfer at four coastal sites  
7           using a chamber method. *Journal of Marine Systems* 66: 140-149.

8   Tokoro, T., H. Kayanne, A. Watanabe, K. Nadaoka, H. Tamura, K. Nozaki, K. Kato,  
9           AND A. Negishi 2008. High gas-transfer velocity in coastal regions with high  
10          energy-dissipation rates. *Journal of Geophysical Research* 113: C11006.

11   Upstill-Goddard, R. C. 2006. Air-sea gas exchange in the coastal zone. *Estuarine,  
12          Coastal and Shelf Science*, 70: 388-404.

13   Wanninkhof, R. 1992. Relationship between Wind Speed and Gas Exchange Over the  
14          Ocean. *Journal of Geophysical Research* 97: 7373-7382.

15   Wanninkhof, R. AND W. R. McGillis 1999. A cubic relationship between air-sea CO<sub>2</sub>  
16          exchange and wind speed. *Geophysical Research Letters* 26: 1889-1892.

17   Watanabe A. 2004. Processes of seawater CO<sub>2</sub> system formation and biological  
18          community metabolism in coral reefs and brackish estuaries. Thesis, University of  
19          Tokyo, pp. 210.

20   Watanabe, A., H. Kayanne, K. Nozaki, K. Kato, A. Negishi, S. Kudo, H. Kimoto, M.  
21          Tsuda, AND A. G. Dickson 2004. A rapid, precise potentiometric determination  
22          of total alkalinity in seawater by a newly developed flow-through analyzer  
23          designed for coastal regions. *Marine Chemistry* 85: 75- 87.

24   Weiss, R. F. 1974. Carbon dioxide in water and seawater: The solubility of a non-ideal

1 gas. *ibid* 2: 203-215.

2 Yamano, H., H. Kayanne, N. Yonekura, H. Nakamura, AND K. Kudo 1998. Water  
3 circulation in a fringing reef located in a monsoon area: Kabira reef, Ishigaki  
4 Island, Southwest Japan. *Coral Reefs* 17: 89-99.

5 Yamano, H., H. Kayanne, N. Yonekura, AND K. Kudo 2000. 21-year changes of  
6 backreef coral distribution: Causes and significance. *Journal of Coastal Research*  
7 16: 99-110.

8 Zappa, C. J., P. A. Raymond, E. A. Terray, AND W. R. McGillis 2003. Variation in  
9 surface turbulence and the gas transfer velocity over a tidal cycle in a macro-tidal  
10 estuary. *Estuaries* 26: 1401-1415.

11 Zappa, C. J., W. R. McGillis, P. A. Raymond, J. B. Edson, E. J. Hinst, H. J.  
12 Zemmeling, J. W. H. Dacey, AND D. T. Ho 2007. Environmental turbulence  
13 mixing controls on air-water gas exchange in marine and aquatic systems.  
14 *Geophysical Research Letters* 34: L10601.

15

1 Table 1. Calculated  $k_{w,600}$ , averages of wind speed ( $U_{10}$ ) and water depth. Wind speeds  
 2 and water depths were averaged values during residence time of reef water. The data  
 3 during daytime is indicated as italic.

Date and Time (LT)	$k_{w,600}$ (cm h <sup>-1</sup> )	$U_{10,avg}$ (m s <sup>-1</sup> )	Tide <sub>avg</sub> (m)	Date and Time	$k_{w,600}$ (cm h <sup>-1</sup> )	$U_{10,avg}$ (m s <sup>-1</sup> )	Tide <sub>avg</sub> (m)
<i>Mar 7, 2008</i>				<i>Mar 8, 2008</i>			
0:00	74	7.4	1.45	0:00	57	8.7	1.66
2:00	36	8.0	1.01	1:00	39	8.3	1.44
4:00	52	8.5	0.74	2:00	37	8.5	1.23
6:00	75	9.4	0.92	3:00	40	8.6	1.02
8:00	50	9.7	1.53	4:00	37	8.8	0.87
9:20	30	9.1	1.76	6:00	68	8.8	0.95
10:00	43	9.3	1.83	7:00	64	9.1	1.18
11:00	47	9.1	1.80	9:00	<i>165</i>	8.1	1.67
12:00	<i>-51</i>	8.4	1.62	10:00	<i>127</i>	8.1	1.80
13:00	<i>-28</i>	7.6	1.39	11:00	<i>-5</i>	7.3	1.81
14:00	<i>-17</i>	7.6	1.12	12:00	<i>-1170</i>	7.5	1.67
15:00	<i>0</i>	8.2	0.84	13:00	<i>-323</i>	7.5	1.40
16:00	<i>18</i>	8.5	0.74	14:00	<i>-403</i>	8.1	1.17
17:00	<i>-5</i>	9.2	0.74				
18:00	<i>7</i>	9.2	0.82				
19:00	<i>58</i>	9.1	1.07				
20:00	<i>45</i>	<i>9.5</i>	<i>1.39</i>				
22:00	32	8.7	1.74				
23:00	40	8.6	1.74				

4

1 **Figure legends**

2 Figure 1. Study site.

3

4 Figure 2. Geographical map and current trajectories (solid lines with filled circles) of  
5 the Kabira Reef. Filled circles represent buoy observation point determined by GPS.

6 Filled stars (M800 and W400) represent points where current meter were situated. At  
7 the point E350 inside the reef (filled square), meteorological and oceanographical  
8 observations and water sampling were conducted. Open square located outside the reef  
9 represents the point of water sampling for offshore water.

10

11 Figure 3. Variations of meteorological and oceanographic observations. a) Horizontal  
12 wind vectors; b) salinity; c) water depth at sampling point (E350; d) current vectors at  
13 the reef crest (M800; d) and sampling point (e); f) saturation degree of dissolved  
14 oxygen; g) normalized concentration of dissolved inorganic carbon; h) normalized total  
15 alkalinity; i) fugacity of CO<sub>2</sub> calculated from DIC and TA data. Horizontal lines and  
16 filled symbols in g, h and i represent values at offshore, respectively.

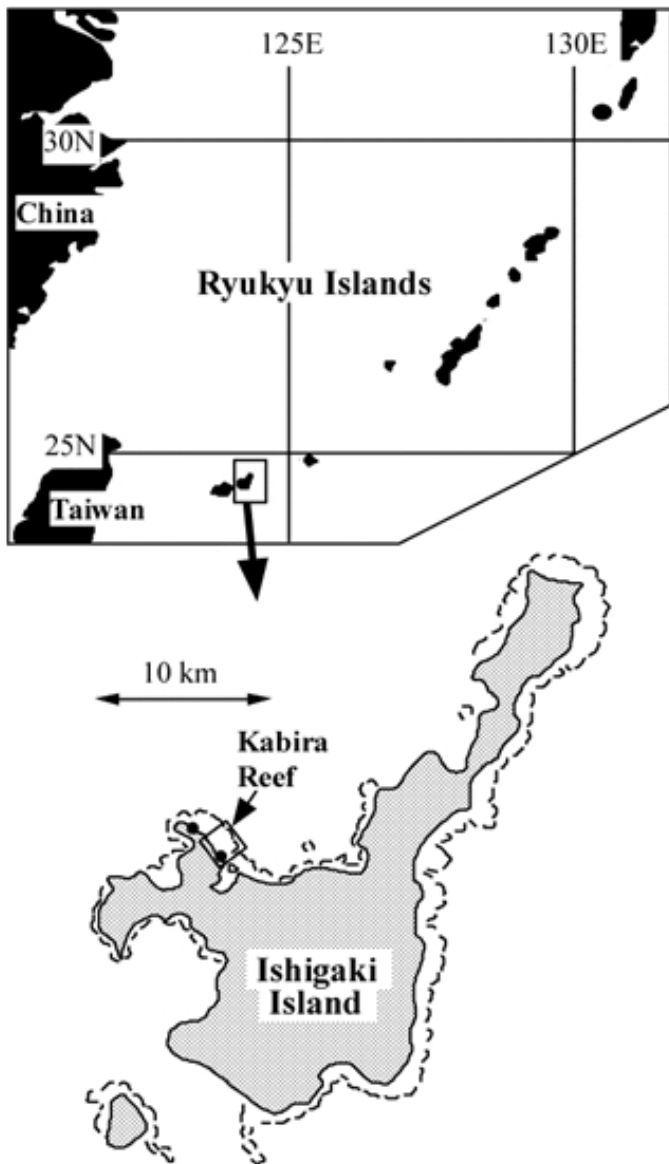
17

18 Figure 4. a) Variation of estimated residence time of reef water (solid line). Filled  
19 diamonds represent observation using drifting buoy experiments. Dashed line indicates  
20 the variation of average depth of the water trajectory. Error bar (0.06 h) represents the  
21 estimated error (5.8% in 1 S. D.) on the average residence time (1.1 h). b) Net  
22 community production (NCP) based on the variation of DIC and TA (filled squares) and  
23 air-sea CO<sub>2</sub> flux to the atmosphere (open diamonds). Shaded area represents irradiance.

24

1 Figure 5. Relationship between transfer velocity normalized to Schmidt number 600 and  
2 horizontal wind speed 10 m above sea level. Open triangles and squares represent  
3 observed values at low and high tides, respectively. Filled triangle and square represent  
4 those averages. The average value during high tide excluded an outlying value during  
5 the lowest wind (upper-right). Error bar ( $4 \text{ cm h}^{-1}$ ) represents the estimated relative error  
6 (9.3 % in 1 S. D.) on the average value during high tides ( $43 \text{ cm h}^{-1}$ ). Solid line  
7 represents an regression by Raymond and Cole (2001) based on non-dome observations  
8 at estuaries and coasts. Long-dashed line represents the result at Hudson River by  
9 Marino and Howarth (1993). Dash-dotted and dotted lines represent wind-dominant  
10 schemes studied previously. Small box represents the result by Tokoro et al. (2008) at  
11 Fukido Reef (gray triangles) and River (gray squares), Ishigaki Island. Lines in the box  
12 represent same regressions as Large box for the horizontal wind speed from 2 to  $5 \text{ m s}^{-1}$ .  
13

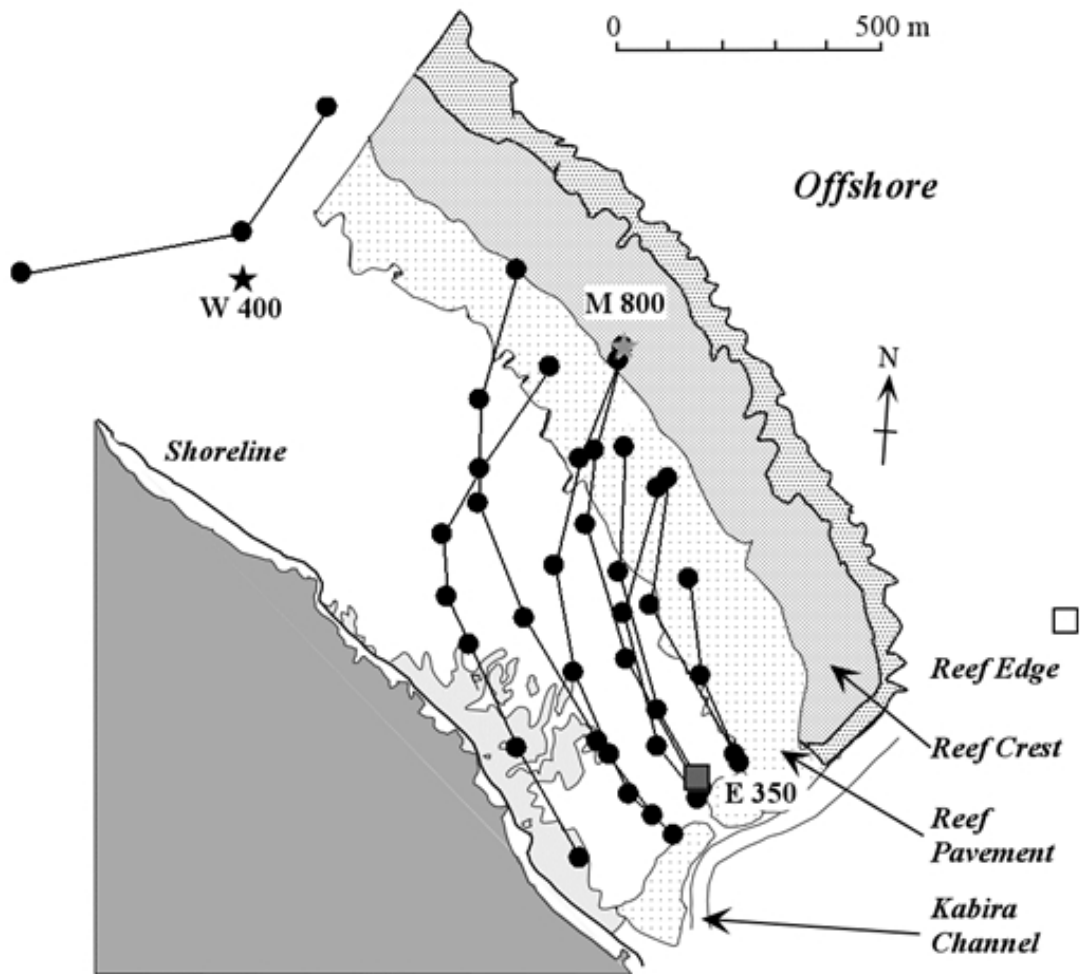




1

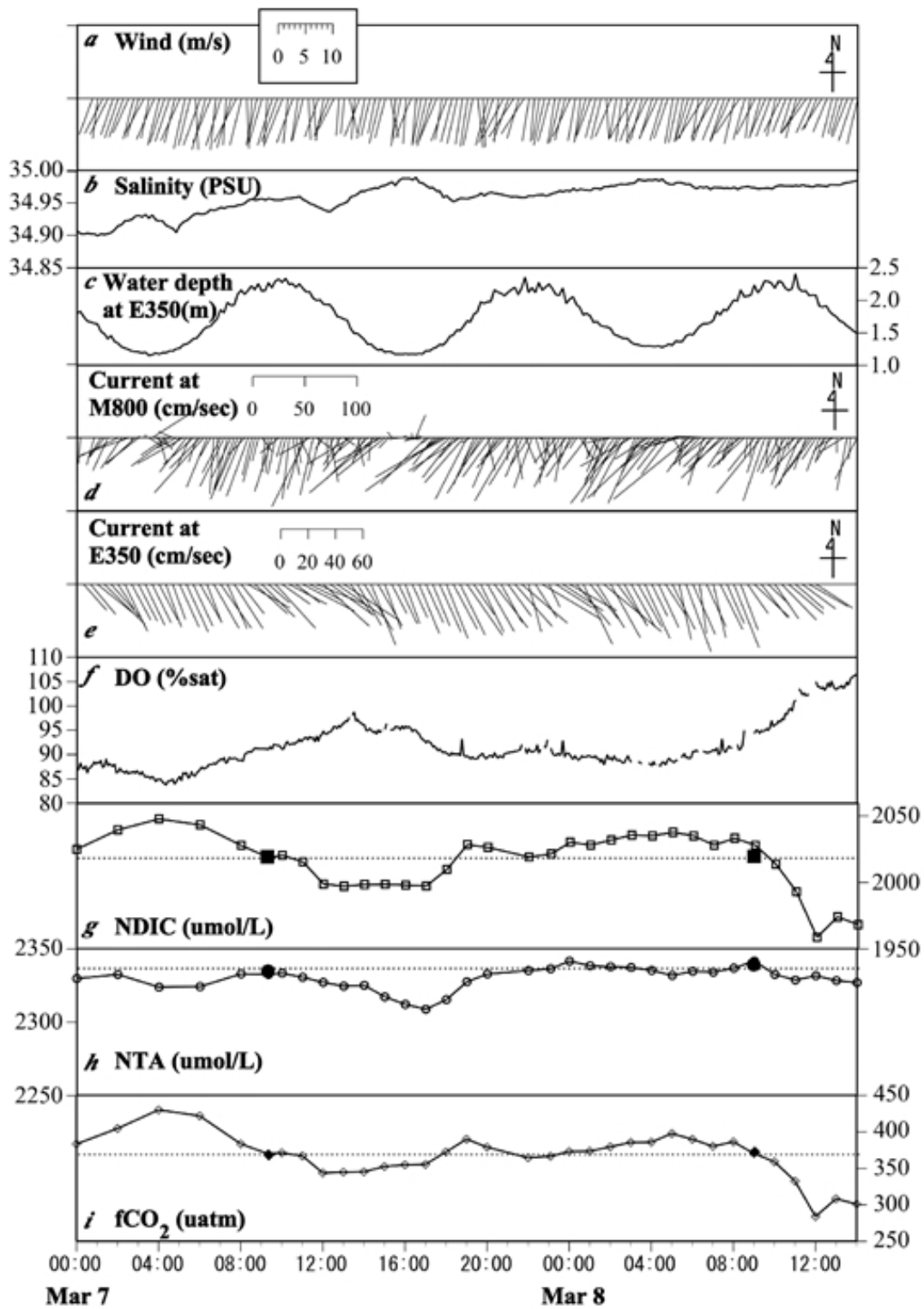
2 Figure 1. Study site.

3



1  
 2 Figure 2. Geographical map and current trajectories (solid lines with filled circles) of  
 3 the Kabira Reef. Filled circles represent buoy observation point determined by GPS.  
 4 Stars (M800 and W400) represent points where current meter were situated. At the  
 5 point E350 inside the reef, meteorological and oceanographical observations and water  
 6 sampling were conducted. Another square symbol outside the reef represents the point  
 7 of water sampling for offshore water.

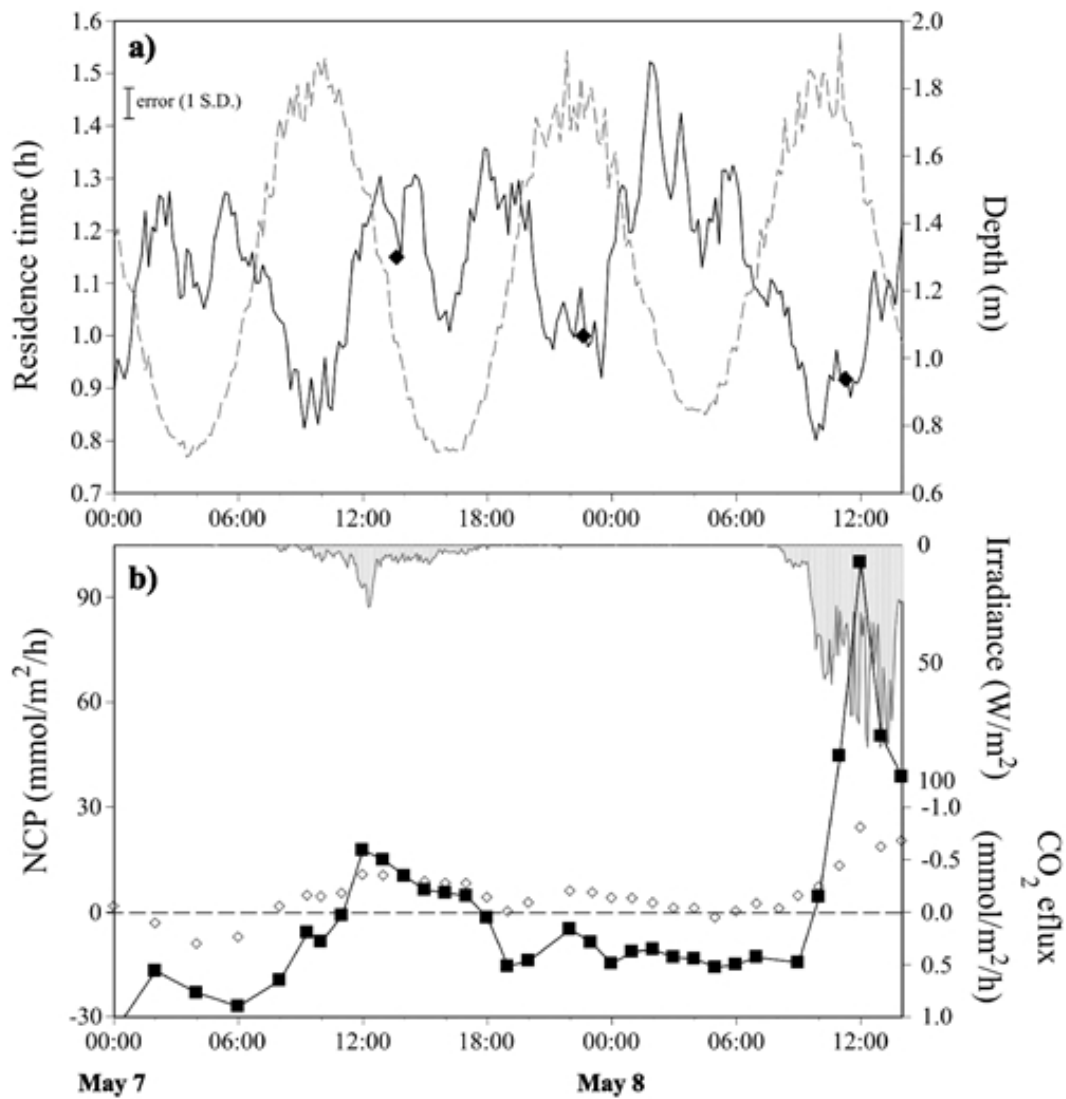
8



1

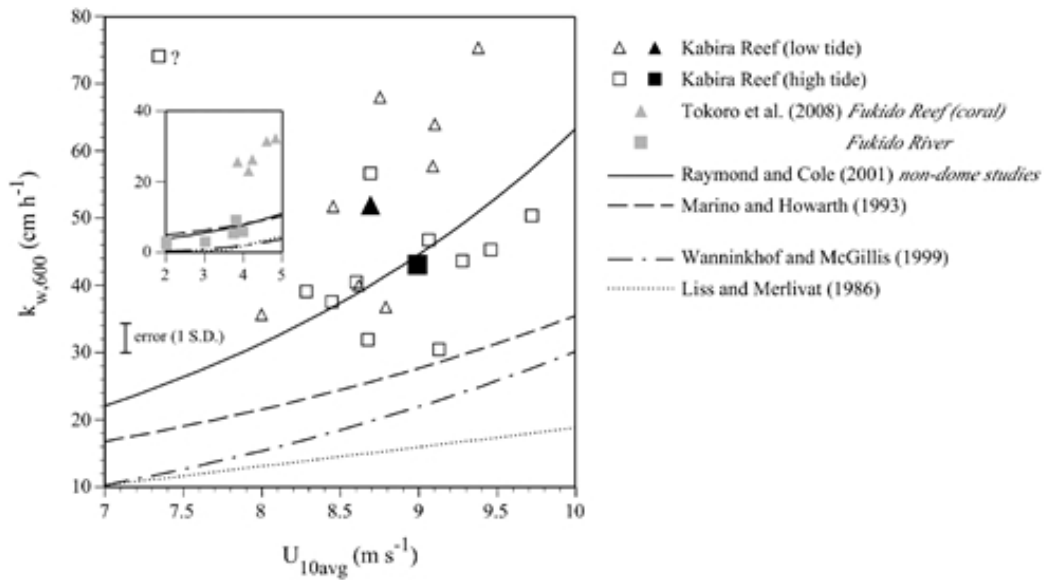
2

1 Figure 3. Variations of meteorological and oceanographic observations. a) Horizontal  
2 wind vectors; b) salinity; c) water depth at sampling point (E350; d) current vectors at  
3 the reef crest (M800; d) and sampling point (e); f) saturation degree of dissolved  
4 oxygen; g) normalized concentration of dissolved inorganic carbon; h) normalized total  
5 alkalinity; i) fugacity of CO<sub>2</sub> calculated from DIC and TA data. Horizontal lines and  
6 filled symbols in g, h and i represent values at offshore, respectively.



1

2 Figure 4. a) Variation of estimated residence time of reef water (solid line). Filled  
 3 diamonds represent observation using drifting buoy experiments. Dashed line indicates  
 4 the variation of average depth of the water trajectory. Error bar (0.06 h) represents the  
 5 estimated error (5.8% in 1 S. D.) on the average residence time (1.1 h). b) Net  
 6 community production (NCP) based on the variation of DIC and TA (filled squares) and  
 7 air-sea CO<sub>2</sub> flux to the atmosphere (open diamonds). Shaded area represents irradiance.



1  
 2 Figure 5. Relationship between transfer velocity normalized to Schmidt number 600 and  
 3 horizontal wind speed 10 m above sea level. Open triangles and squares represent  
 4 observed values at low and high tides, respectively. Filled triangle and square represent  
 5 those averages. The average value during high tide excluded an outlying value during  
 6 the lowest wind (upper-right). Error bar ( $4 \text{ cm h}^{-1}$ ) represents the estimated relative error  
 7 ( $9.3\%$  in 1 S. D.) on the average value during high tides ( $43 \text{ cm h}^{-1}$ ). Solid line  
 8 represents an regression by Raymond and Cole (2001) based on non-dome observations  
 9 at estuaries and coasts. Long-dashed line represents the result at Hudson River by  
 10 Marino and Howarth (1993). Dash-dotted and dotted lines represent wind-dominant  
 11 schemes studied previously. Small box represents the result by Tokoro et al. (2008) at  
 12 Fukido Reef (gray triangles) and River (gray squares), Ishigaki Island. Lines in the box  
 13 represent same regressions as Large box for the horizontal wind speed from  $2$  to  $5 \text{ m s}^{-1}$ .  
 14